THE ASTRONOMICAL JOURNAL, 117:102–110, 1999 January

CONSTRAINTS ON THE EARLY FORMATION OF FIELD ELLIPTICAL GALAXIES

A. J. BARGER,[1,2] L. L. COWIE,[1] N. TRENTHAM,[3] E. FULTON,[1,2] E. M. HU,[1] A. SONGAILA,[1] AND D. HALL[1]

Received 1998 May 29; accepted 1998 September 22

ABSTRACT

We present the results of an HK' wide-field survey encompassing the Hubble Deep Field and its flanking fields. Our wide-field survey provides uniform coverage of a 61.8 arcmin^2 area to a depth equivalent to $K = 20.1$ at 5 σ. We have also imaged the Hubble Deep Field in HK', providing uniform coverage of a 7.8 arcmin^2 area to a depth equivalent to $K = 21.2$ at 5 σ. Using these data in combination with new deep University of Hawaii 8K V and I imaging obtained on the Canada-France-Hawaii Telescope, we find only a small population of objects with colors redder than an equivalent $I-K = 4$, the color expected for an evolved elliptical galaxy at $z > 1$. We infer that only a fraction of the local field elliptical galaxy population with $M_K < -23.4$ could have formed in single bursts at high redshift.

Key words: cosmology: observations — galaxies: evolution — galaxies: photometry

1. INTRODUCTION

The study of galactic evolution is a primary area of observational cosmology because it is central to understanding the nature of galaxies and to probing the cosmological geometry. With observational data now revealing normal galaxies at redshifts as high as $z \sim 5$, we should be close to being able to locate or rule out the existence of a substantial high-redshift field elliptical galaxy population. These old systems would have formed at the earliest times, and hence their existence would place very stringent constraints on galaxy and structure formation.

How elliptical galaxies formed remains a topic of debate. The standard view (e.g., Eggen, Lynden-Bell, & Sandage 1962; Tinsley & Gunn 1976) has been that elliptical galaxies formed the bulk of their stars in a single burst of star formation at high redshift, after which their stellar populations evolved passively. This monolithic collapse model for elliptical formation is in marked contrast with the hierarchical merging scenario for galaxy formation and evolution, in which massive galaxies form at all redshifts from the gradual merging of smaller galaxies (e.g., White & Frenk 1991; Kauffmann, White, & Guiderdoni 1993; Baugh, Cole, & Frenk 1996). The monolithic collapse model appears to be supported by extensive studies of elliptical galaxies in rich cluster environments to $z > 1$. Observational studies of the color evolution in cluster early-type galaxies have demonstrated that the changes with redshift are consistent with a model in which stellar populations formed at high redshift, $z_f > 2$, and subsequently evolved passively (e.g., Aragón-Salamanca et al. 1993). A similar $z_f > 2$ constraint is obtained from the observed small scatter in the color-magnitude relations in distant clusters (see, e.g., Ellis et al. 1997; Stanford, Eisenhardt, & Dickinson 1995, 1998), and from the evolution of the Mg b versus σ relation (e.g., Ziegler & Bender 1997) and the fundamental plane relation (e.g., Dokkum & Franx 1996; Kelson et al. 1997). However, Kauffmann & Charlot (1998) have argued that in the rich cluster environment hierarchical elliptical galaxy evolution may appear indistinguishable from that predicted by the passive evolution scenario. In their model, rich clusters at high redshift correspond to regions where the very earliest star formation occurred, and hence the star formation and merging histories of galaxies in these clusters have progressed much further than have those of field galaxies. Thus, in observing apparently similar clusters of galaxies, observers may be selecting only the oldest galaxies at any particular redshift.

Because the passive evolution scenario for elliptical galaxies predicts a population of $z > 1$ galaxies with ultrared optical–near-IR colors, this scenario can be sensitively tested in the field environment with very deep optical and near-infrared imaging surveys. Low-redshift galaxies with significant star formation can mimic the very red colors of an evolved elliptical galaxy if they are greatly reddened by dust. However, the number of ultrared objects observed gives an *upper* limit on the comoving number density of passively evolving elliptical galaxies, provided that there does not exist a population of completely dust-obscured high-redshift objects. Imaging surveys have only recently become deep enough in both the optical and the near-IR bands to test for the presence of ultrared galaxies at $z > 1$.

Cowie et al. (1994) presented a very deep K-band survey of four small fields of total area 5.9 arcmin^2, which they later followed up spectroscopically (Songaila et al. 1994). From their data they found that the space density of extremely red objects having $I-K > 4$, the expected color for old stellar populations at $z > 1$, implied that at most 10% of the total local galaxy population could have formed in early single-starburst events. A comparison of their $K < 20.9$ sample with a wider, brighter sample having $K < 17.8$ also showed a scarcity of very red objects that could lie at redshifts $z > 1$. Thus, Cowie et al. suggested that either galaxies are less luminous at these higher redshifts or the mix of galaxy types is much bluer than expected. Recently, Hogg et al. (1997) and Moustakas et al. (1997) analyzed a few very deep, small-area fields in K. Hogg et al. imaged two subfields ($\sim$1 arcmin^2 total area) in the Hubble Deep Field (HDF; Williams et al. 1996) with the Near Infrared Camera on Keck to a 90% completeness limit of $K = 23$. Most of their sources had colors consistent with either old stellar populations observed at $0 < z < 1$ or

[1] Institute for Astronomy, University of Hawaii, 2680 Woodlawn Drive, Honolulu, HI 96822.

[2] Visiting Astronomer, Canada-France-Hawaii Telescope, operated by the National Research Council of Canada, the Centre National de la Recherche Scientifique of France, and the University of Hawaii.

[3] Institute of Astronomy, University of Cambridge, Madingley Road, Cambridge CB3 0HA, England, UK.

younger populations observed over a wide range of redshifts. However, they also found four sources that had very red colors, $I_{814}-K > 4$. Moustakas et al. presented colors for very faint galaxies ($K < 23$) in two fields covering an area ~ 2 arcmin^2. They found a small population of galaxies in their sample whose infrared-bright ($I-K > 4$) but relatively blue optical ($V-I \lesssim 2.5$) colors could not be reproduced with any of their standard models. Moustakas et al. suggested three possible scenarios to explain these "red outliers," namely, (i) a universal event of secondary bursts in $z \sim 3$ passively evolving elliptical galaxies; (ii) a combination of very low metallicity and substantial reddening in $z < 1.5$ galaxies; or (iii) the existence of dusty, old populations within the galactic nuclei of normal galaxies. In their preliminary follow-up analysis, Moustakas et al. (1998) presented *HST* WFPC2 and NICMOS morphologies for some of their red outliers. These images showed the objects to be compact and asymmetric and hence unlikely to be relaxed systems. Thus, these authors now prefer the explanation that the red outlier population consists of very dusty $z > 1.2$ systems containing bright nuclei powered by either AGNs or starbursts. In the present paper, we find that such objects are much rarer than was measured by Moustakas et al.

The results of the above three surveys, as well as those from recent K-band HDF imaging by Dickinson et al., were subsequently analyzed by Zepf (1997) to determine the dominant formation mechanism for elliptical galaxies. Zepf compared the observed surface densities of the ultrared galaxies to a given magnitude limit with their expected surface densities, assuming a passive formation model in which all early-type galaxies form in short bursts at high redshift. He concluded that there is a strong deficit of galaxies with extremely red colors in the observed fields (therefore ruling out models where typical elliptical galaxies are fully assembled and have formed all of their stars by $z > 5$), and thus that most elliptical galaxies must have formed at $z < 5$ through merging and associated starbursts.

Using the HDF data set of Dickinson et al., Franceschini et al. (1998) analyzed the spectral energy distributions of morphological elliptical galaxies in the HDF to date the dominant stellar populations. They found that the majority of the bright early-type galaxies are at $z \lesssim 1.3$ and have colors that indicate ages of typically 1.5–3 Gyr. The sudden disappearance of objects at $z > 1.3$, when the objects should have been visible in a luminous star formation phase, is explained by Franceschini et al. as being due to the fact that during the first few Gyr of the galaxy's lifetime the objects are undergoing dust-enshrouded merger-driven starbursts.

Provided that high-redshift elliptical galaxies are not completely obscured by dust, deep infrared surveys can detect their presence and place constraints on their surface density. Existing deep K-band surveys have concentrated on small areas due to the small format of the IR arrays. However, with the development of large-format IR arrays such as the 1024 × 1024 pixel HgCdTe Astronomical Wide Area Infrared Imaging (HAWAII) devices, it is now feasible to conduct deep near-infrared surveys over wider fields. In this paper, we present a wide-field HK' survey of the HDF and its flanking fields with corresponding V and I colors. The primary goal of our imaging survey is to compile a well-defined sample of near-infrared selected galaxies over a large area to place constraints on the population of ultrared galaxies. As a complement to this wide-field survey, we also have obtained very deep HK'-band observations of the HDF itself.

In § 2 we describe our new data sample and the construction of our photometric catalogs. In § 3 we use our imaging data to study galaxy colors and the effects of dust, and in § 4 we use our data to put constraints on the high-redshift field elliptical galaxy population. Section 5 summarizes our results.

2. DATA

2.1. *Observations*

To complement the multicolor data of the HDF, we have obtained deep follow-up HK' observations of the HDF and its flanking fields using the University of Hawaii (UH) 2.2 m telescope and the 3.6 m Canada-France-Hawaii Telescope (CFHT). We have also obtained deep V- and I-band observations with the CFHT over a much larger area and Keck Low Resolution Imaging Spectrograph B-band observations in a strip across the center of the HK' wide-field image.

The wide-field near-infrared images were obtained with the UH 2.2 m telescope on the nights of UT 1997 April 17–22 using the University of Hawaii Quick Infrared Camera (QUIRC; Hodapp et al. 1996). QUIRC utilizes a 1024 × 1024 pixel HAWAII array produced by the Rockwell International Science Center. At the f/10 focal ratio, the field of view of QUIRC is 193 arcsec square with a scale of 0.″1886 pixel^{-1}. The observations were made using a notched HK' filter with a central wavelength of 1.8 μm (Wainscoat & Cowie 1999). The filter covers the longer wavelength region of the H band and the shorter wavelength region of the K band (roughly the K' filter). Because of its broad bandpass and low sky background, this filter is extremely fast and is roughly twice as sensitive as the H, K', or K_s filters. We covered the full area imaged with the *HST* using a 3 × 3 mosaic with a 20″ overlap. Thirteen spatially shifted short exposures (around 100 s each depending on the background level) of step size 5″–20″ in all directions were obtained at each of the nine pointings within the full mosaic, and the mosaic pattern was repeated several times during the run. This observing strategy enabled us to use the data images for the subsequent sky subtraction and flat-fielding procedures. Each object is sampled by a different array pixel on each exposure, and the signal-to-noise ratio should improve as the square root of the number of frames. The dark current is insignificant in the QUIRC data. The data were processed using median sky flats generated from the dithered images and calibrated from observations of UKIRT faint standards taken on the first three nights when the sky was photometric. The FWHM on the total composite image was 0.″8. The magnitudes were measured in 3.″0 diameter apertures and corrected to total magnitudes following the procedures of Cowie et al. (1994).

Since we will want to compare our HK' measurements with previous K-band data, we need a conversion between the two bands. From K, HK', and I images of galaxies in the SSA 13 field, we find the empirical relation $HK'-K = 0.13 + 0.05(I-K)$. Figure 1 shows $HK'-K$ versus $I-K$ colors for a range of redshifts and galaxy types in the SSA 13 field. The offset between the galaxies and the lone star in the figure reflects the different shapes of stars and galaxies in the wavelength region 1.5–2.4 μm. Stars rise to shorter wavelengths, whereas galaxies are flatter, so even

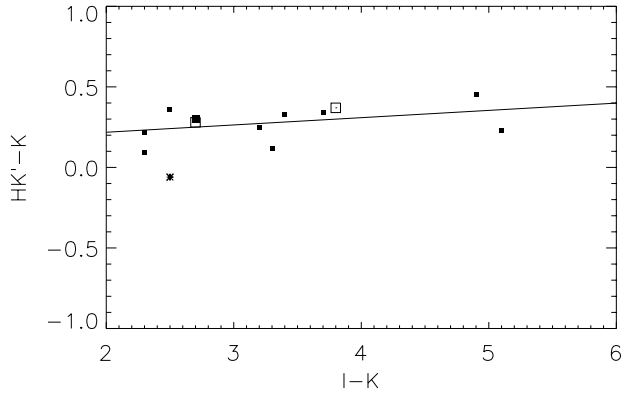

FIG. 1.—$HK'-K$ vs. $I-K$ for objects in the Hawaii Deep Survey Field SSA 13: stars (*star symbol*; only one) and galaxies with magnitudes $K < 18$ (*open squares*), $K = 18$–19 (*large filled square*; only one), and $K = 19$–20 (*small filled squares*). The galaxy color equation obtained from these data is $HK'-K = 0.13 + 0.05(I-K)$.

blue galaxies are offset from stars. Since the coefficient of the $I-K$ term is small, it suffices for us to use a median value for $I-K$ in this relation, and we therefore obtain $HK'-K = 0.30$.

Deep imaging of the HDF itself was obtained in the HK' filter with QUIRC on the UH 2.2 m telescope on the nights of UT 1996 February 6–8 and with QUIRC on the CFHT on the nights of UT 1996 April 5–8. The CFHT image was registered to the UH 2.2 m data, and a noise-weighted addition was performed. The net image quality is $\sim 1''$ FWHM. The noise in each field was estimated by measuring corrected $3''$ diameter magnitudes at a number of blank sky positions. The 2 σ limit for the wide-field image is $HK' = 21.4$ and for the deep image is $HK' = 22.5$.

The V and I optical images were obtained on the nights of UT 1997 April 3–8 with the CFHT and the UH 8K CCD Mosaic Camera, a 2×4 array of 4096×2048 CCDs built by Metzger, Luppino, and Miyazaki. The image scale is $0''.21$ pixel^{-1}. The observations were made through Kron-Cousins I and Johnson V filters and comprise 22 1200 s I-band exposures (8.3 hr) and 33 1200 s V-band exposures (11 hr) under conditions of mixed transparency. Net image quality is $\sim 0''.9$ FWHM in I and $\sim 1''.0$ FWHM in V. The UH 8K data were processed in the standard way using the IMCAT data reduction routines written by N. Kaiser.[4] The data were calibrated to total Kron-Cousins I and Johnson V magnitudes using shallower images obtained under photometric conditions with the UH 2.2 m telescope. The 2 σ limit for the I-band image is $I = 24.8$ and for the V-band image is $V = 25.8$.

2.2. *Photometric Measurements and Catalogs*

Objects were detected and measured on all the images using the SExtractor package written by Bertin & Arnouts (1996). Before extraction the data were convolved with a Gaussian chosen to have an FWHM approximately equal to the seeing. Objects were extracted if they contained at least 25 connected pixels each with a signal above a threshold of 1 σ. The photometric measurements were then made on the unconvolved images using $3''$ diameter apertures, with the photometric calibration described in § 2.1, and corrected to $6''$ diameter magnitudes (Cowie et al. 1994). All magnitudes presented in this paper are given as these near total magnitudes.

We determined the incompleteness of the wide-field HK' catalog by measuring objects in the wide-field image at the positions of the deep near-infrared catalog. By comparing the fraction of galaxies already included in the wide-field HK' sample with those measured using the deep HK' catalog as a function of near-infrared magnitude, we found that the wide-field near-infrared catalog became more than 50% incomplete at $HK' \gtrsim 21.3$. We further checked the incompleteness of the wide-field near-infrared catalog, and determined the incompleteness of the deep HK' field, by constructing I and V samples with SExtractor (as above). We measured photometry at the optical positions on the near-infrared images. We compared the fraction of galaxies already included in the HK' sample with those measured using the optically selected catalogs as a function of near-infrared magnitude and found a consistent incompleteness level for the wide-field near-infrared catalog with what we found above. The deep catalog became more than 50% incomplete at $HK' \gtrsim 22.3$.

To determine the J2000 coordinates for our HK'-selected sample, we first obtained the plate scale and the orientation angle for the QUIRC camera using our wide-field HK' image. We chose to use the Automatic Plate Measuring Facility (APM) eo674 plate, where our field is slightly more centered. From a fit to 33 APM objects ($17 < V < 22.5$) covering our field, we found a plate scale of $0''.189$ pixel^{-1} and an orientation angle of $0°.636$ north through east, both of which are consistent with previous determinations for the QUIRC camera (the orientation angle was previously determined to be $0°.728$ for B1950). The dispersion of the fit was $0''.32$ in both the right ascension and declination directions, giving a total error of $0''.45$. This error is comparable to the expected astrometric errors in the APM catalog. As a check, we compared the right ascension and declination positions in the two APM plates covering the region (eo1427 and eo674) and found an rms error between the two plates of $0''.73$. The average offsets of $1''.8$ in R.A. and $1''.5$ in decl. between the positions measured from the two plates are consistent with the APM errors that fully dominate the error budget. (Our field lies close to the edge of the eo1427 plate where the APM solution may be worse.) Futhermore, the offsets are consistent with the advertised accuracies of the APM absolute astrometry. No systematic effects were visible.

The offsets to the Very Large Array (VLA) system, determined using the five radio sources in Fomalont et al. (1997) that have the smallest right ascension and declination errors ($0''.2$) from their identified $I < 22$ optical counterparts, were found to be $1''.68$ in the right ascension direction and $-0''.59$ in the declination direction, consistent with the expected APM absolute errors. The rms errors of $0''.16$ in the right ascension direction and $0''.11$ in the declination direction are consistent with the radio source errors.

The wide-field catalog of HK'-selected objects whose centers fall within an area ~ 7.9 arcmin^2, the region over which the coverage is uniform, has been posted to a web page linked to the Hubble Deep Field Clearing House page at STScI. For each object we give a right ascension and declination catalog number, a J2000 right ascension and declination tied to the VLA coordinates of Fomalont et al. (1997) (described above), and our HK', Kron-Cousins I,

[4] The IMCAT software may be obtained by contacting N. Kaiser at kaiser@hawaii.edu.

Johnson V, and, where available, B total magnitudes. Ground-based spectroscopic survey observations of galaxies in the HDF have been taken with the Keck telescope and either published or made publicly available by several groups (Cohen et al. 1996; Steidel et al. 1996; Lowenthal et al. 1997; Phillips et al. 1997; the Hawaii Active Catalog of the HDF[5]). These spectroscopic redshifts are included in the catalog.

2.3. *Star-Galaxy Separation*

Stars are cleanly separated from galaxies in the $B-I$ versus $I-K$ plane. The $I-K$ colors are primarily a redshift diagnostic. As the redshift increases the ultraviolet part of the galaxy spectrum shifts into the I band, and the $I-K$ colors become progressively redder. On the other hand, $B-I$ colors are primarily a diagnostic of galaxy morphology. The empirical star-galaxy separation line has been found to be $(B-I)-2.5(I-K)=-2.0$ (Kron 1980; Gardner 1992; Huang et al. 1997). For the objects in our data sample for which we have B-band data ($\sim 50\%$), this line, converted to HK', also provides an appropriate star-galaxy separation. We determine a corresponding separation line in $V-I$ versus $I-HK'$ that reproduces the above star or galaxy classifications $[(V-I)-2.0(I-HK')=-1.1]$ and apply it to classify the remaining objects in our wide-field sample (see Fig. 3).

3. GALAXY COLORS IN THE NEAR-INFRARED SAMPLES

In Figure 2, we show the $I-HK'$ versus HK' and $V-HK'$ versus HK' color-magnitude diagrams (both stars and galaxies) for the 5 σ near-IR selected samples in our wide-field and deep HDF images. Only five of the 664 objects in the 5 σ wide-field sample were not detected at or above the 2 σ level in I, and 41 were not detected at or above the 2 σ level in V. For the deep HDF image, six of the 184 objects in the 5 σ near-IR selected sample were not detected at or above the 2 σ level in I, and 18 were not detected at or above the 2 σ level in V. We assign these objects 2 σ limiting magnitudes for the following analysis, and we mark their $V-HK'$ and $I-HK'$ colors as lower limits on the plots with an upward-pointing arrow. The solid lines show the 2 σ magnitude limits on the $I-HK'$ or $V-HK'$ colors, and the dotted lines in the two $I-HK'$ versus HK' figures indicate our adopted definition of $I-HK'>3.7$ for the ultrared galaxy population, which we shall discuss in detail below.

In Figures 3 and 4, we plot $V-I$ versus $I-HK'$ diagrams for our galaxy samples, letting the size of the symbols decrease with decreasing galaxy brightness. Galaxy evolutionary codes provide a powerful means for interpreting galaxy color-color distributions. To aid in our interpretation of the data, we overlay on the data template model galaxy tracks for three representative star formation histories. These models were produced with the code of G. Bruzual and S. Charlot (1996, private communication, hereafter BC96) assuming solar metallicity, Salpeter initial mass function, and exponentially declining star formation rates. The star formation timescales adopted are $\tau=(0.1, 2, 20)$ Gyr, which roughly approximate elliptical, Sa, and constant star-forming galaxies, respectively. We label the tracks with representative redshifts over the range $0<z<3$ at which the galaxies would be observed. In all our model comparisons with the data, we adopt a $q_0=0.5$ cosmology and a Hubble constant of $H_0=50$ km s^{-1} Mpc^{-1}. Barring modeling uncertainties, galaxies following a particular evolutionary track in the color-color plane should appear scattered about the track by observational uncertainties.

The model curves in Figures 3*a* and 3*b* illustrate the no-evolution scenario in which spectral energy distributions (SEDs) corresponding to local evolved galaxies (modeled with BC96 assuming a common epoch of formation, $z_f=5$) are moved back in redshift. Thus, the tracks represent color changes due to pure K-correction. In the figure, these pure K-correction models are overlaid onto the (*a*) wide-field and (*b*) deep-field HK'-selected samples. Nearly all of our galaxies in both surveys have colors consistent with a $z<1$ population. The deep sample also contains a substantial population of objects consistent with high-z star-forming galaxies. Significantly, however, although there are a number of bright objects with red $V-I$, $I-HK'$ colors consistent with the $z<1$ elliptical galaxy evolution tracks, there are no galaxies following these tracks for $z>1$.

The only possible candidates for $z>1$ pure K-correction elliptical galaxies are galaxies in K-selected field samples found to have extremely red $I-K$ colors. The $I-K$ color of a pure K-correction elliptical becomes very red beyond $z=1$, where the 4000 Å break moves between the I and K bands. Thereafter, the $I-K$ color is a sensitive function of the redshift. The color of a pure K-correction elliptical galaxy at $z=1$ is $I-K\simeq 4$. For consistency with previous surveys, we also select this number as the lower limit for defining the *ultrared* galaxy population. For our HK' sample this cutoff is equivalent to $I-HK'=3.7$. By $z\sim 2$ the $I-K$ color should exceed 6 (i.e., assuming a large redshift of formation), but observed objects this red are extremely rare. The most robust $I-K>6$ detections are those of Hu & Ridgway (1994). They found several K-band–bright galaxies in the field of the quasar PC 1643+4631A (most probably serendipitously discovered field objects) with $I-K\sim 6.5$. Recently, Cimatti et al. (1998) detected one of these objects (HR 10) with the submillimeter bolometer array SCUBA on the James Clerk Maxwell Telescope, thereby demonstrating that HR 10 is a very dusty galaxy undergoing a major episode of star formation.

Moustakas et al. (1997) separated out a population of $I-K\gtrsim 4$ galaxies in their sample having blue optical colors $V-I\lesssim 2.5$ (the "red outliers") and suggested that these objects could be fairly common. To $K\sim 20$ in their sample, two secure objects fall into this category. For their survey area of ~ 2 arcmin^2, this corresponds to a surface density of 3600 deg^{-2}. For comparison, in our wide-field sample to an equivalent $K=20.1$ ($HK'=20.4$), we find 16 objects that could potentially satisfy the red outlier color criteria, which corresponds to a surface density of 900^{1200}_{700} deg^{-2}. Given the fact that we cover a much larger area (61.8 arcmin^2), it seems likely that the Moustakas et al. results may have been an upward statistical fluctuation or a clustering effect, and we conclude that this class of galaxy is rare. (These results should be compared with Cohen et al. [1999], who find 19 objects with $R-K\geq 5$ to $K<20$ in a 14.6 arcmin^2 area.)

Although the ultrared galaxy population does not appear to correspond well with the pure K-correction elliptical track, this region is spanned by some nonevolving spiral curves (e.g., $\tau=2$, which roughly approximates an Sa galaxy) with $z>1$. Songaila et al. (1994) found no evidence

[5] See http://www.ifa.hawaii.edu/~cowie/tts/tts.html.

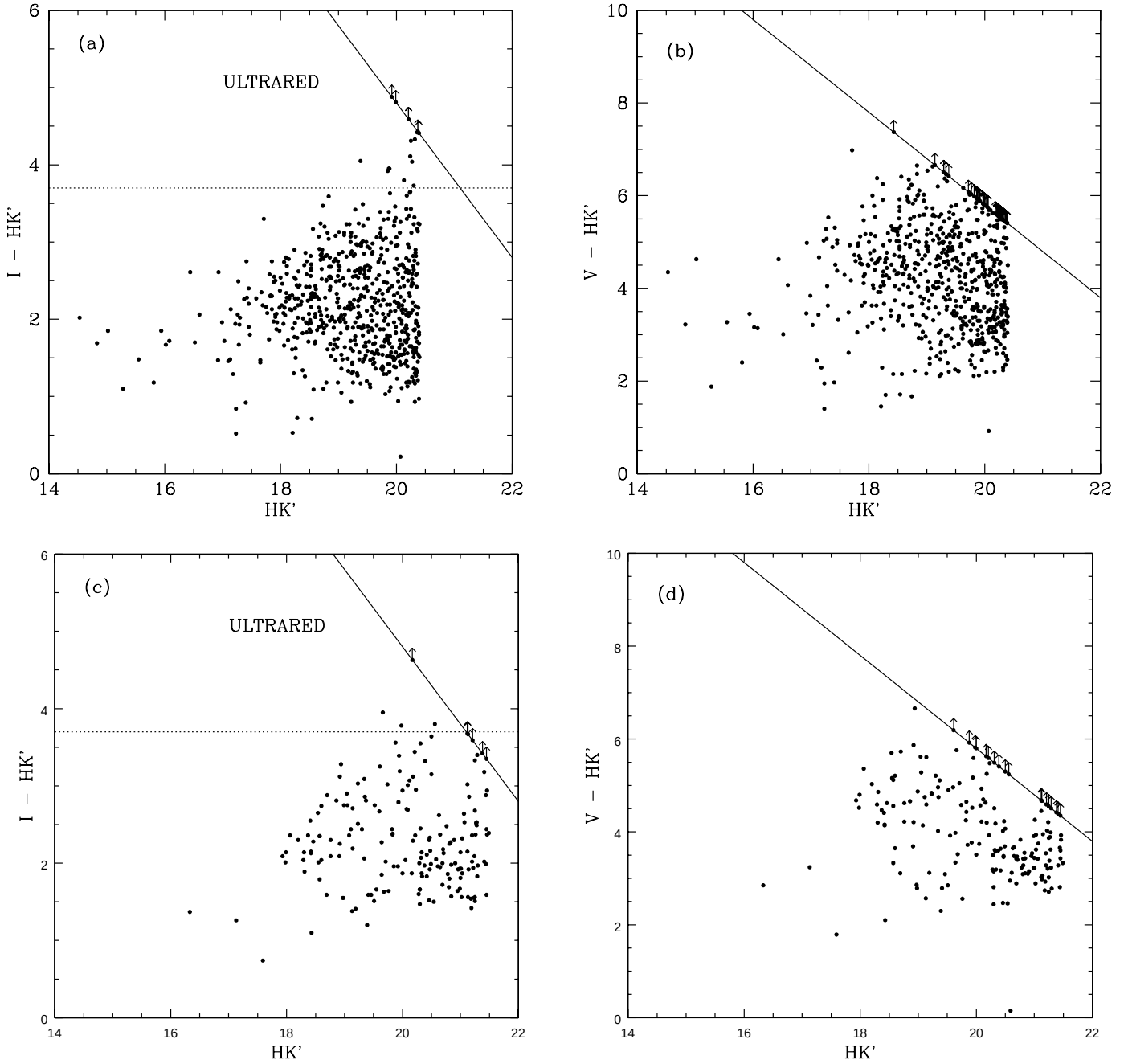

FIG. 2.—Color-magnitude diagrams for the 5 σ HK'-selected sample of objects (stars and galaxies): (*a*) $I-HK'$ vs. HK' and (*b*) $V-HK'$ vs. HK' for the wide-field sample; (*c*) $I-HK'$ vs. HK' and (*d*) $V-HK'$ vs. HK' for the deep sample. The solid lines are 2 σ upper limits on the colors. The dotted lines in (*a*) and (*c*) mark the lower limit for ultrared galaxies ($I-HK' > 3.7$). The upward-pointing arrows represent objects that were undetected at the 2 σ level in I (*a*, *c*) or V (*b*, *d*).

in their $K < 20$ spectroscopic sample of the Hawaii Survey Fields for any ultrared galaxies between $z = 0$ and $z = 1$. They noted that their spectroscopically unidentified objects, many of which appeared to be red $I-K$ objects, had colors that were consistent with being primarily in the redshift interval $z = 1$–2 and falling somewhere between the color of an unevolved Sb and an unevolved Im galaxy.

In Figures 4*a* and 4*b*, we overlay on the wide-field data model curves that trace with redshift the colors of a passively evolving population of galaxies for two different epochs of formation, $z_f = 5$ and $z_f = 3$, respectively. Changing the cosmology to $q_0 = 0.15$, $H_0 = 65$ km s^{-1} Mpc^{-1} makes very little difference in the model tracks. The first thing we notice in this figure is a population of objects at $I-HK' > 3.7$ that appears to fall outside the range of the passively evolving model curves. Although this region does not seem to be well represented by the passively evolving model curves, it may be better described by a reddened elliptical galaxy SED.

In Figure 5, we compare a $z_f = 3$ unreddened, passively evolving $\tau = 0.1$ model galaxy with one reddened using the dust attenuation law of Calzetti (1997) for star-forming galaxies. In the galaxy rest frame, the reddened, $F_{\rm red}(\lambda)$, and intrinsic, $F(\lambda)$, fluxes are related by

$$F_{\rm red}(\lambda) = F(\lambda)10^{-0.4E(B-V)k(\lambda)} . \quad (1)$$

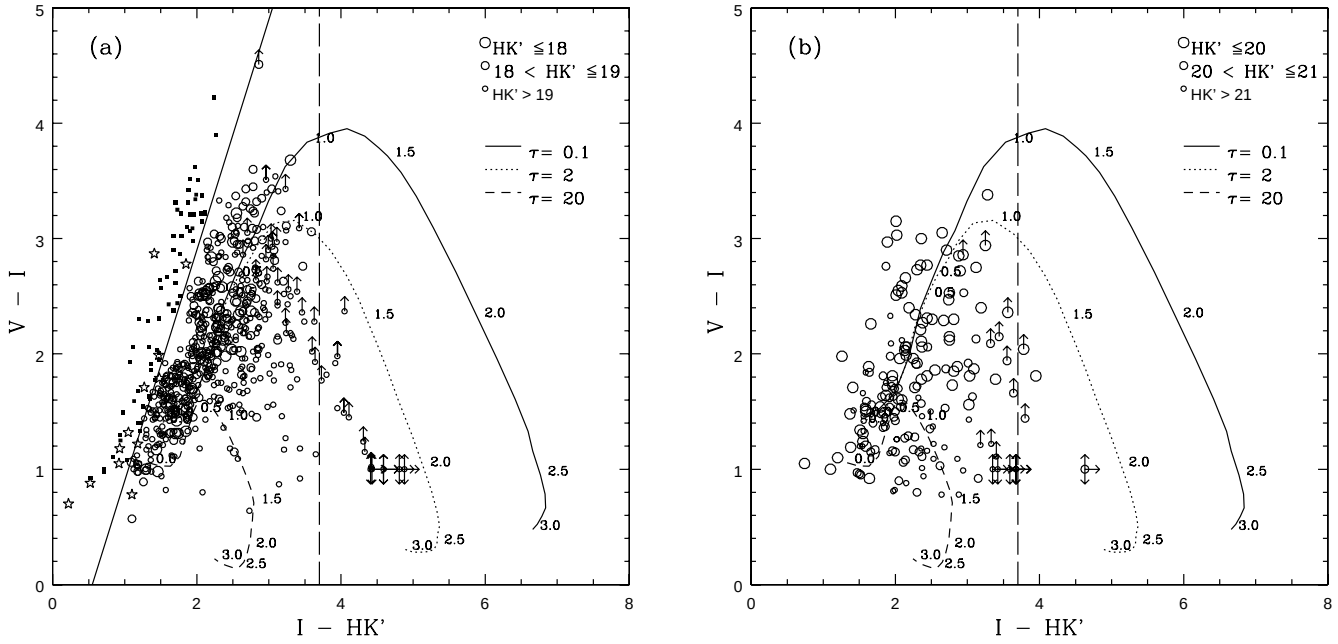

FIG. 3.—$V-I$ vs. $I-HK'$ color-color diagrams for (*a*) the wide-field $HK' \leq 20.4$ sample and for (*b*) the deep HDF $HK' \leq 21.5$ sample. The BC96 pure K-correction model tracks folded with the appropriate V, I, and HK' filters are illustrated from $0 < z < 3$, assuming a common epoch of formation $z_f = 5$. The model tracks have been labeled with a few representative redshifts at which the various colors would be observed. In (*a*) the adopted star-galaxy separation line determined in § 2.3 is indicated by a solid line. The star symbols are definite stars identified either by spectroscopy or from the *HST* images. The filled squares are objects assumed to be stars based on their location above the star-galaxy separation line in the color-color plane. All objects classified as stars were removed from the wide-field sample for the analysis. No stars were removed from the deep sample. The vertical dashed lines in the figures illustrate the ultrared dividing line, $I-HK' > 3.7$.

In Calzetti's recipe for reddening, the attenuation of the stellar continuum, $k(\lambda)$, is given by

$$k(\lambda) = [(1.86 - 0.48/\lambda)/\lambda - 0.10]/\lambda + 1.73 \qquad (2)$$

for $0.63\ \mu\text{m} \leq \lambda \leq 1.0\ \mu\text{m}$, and

$$k(\lambda) = 2.656(-2.156 + 1.509/\lambda - 0.198/\lambda^2 + 0.011/\lambda^3) + 4.88 \qquad (3)$$

for $0.12\ \mu\text{m} \leq \lambda < 0.63\ \mu\text{m}$. Our illustration in Figure 5 is based on a color excess of $E(B-V) = 0.3$.

The reddening law above incorporates the effects of extinction and scattering, as well as the geometrical distribution of the dust relative to the emitters. We can only apply this relation over the redshift range $1.5 < z < 3.0$ because of her wavelength restrictions.

The BC96 models show that a $\tau = 0.1$ star formation

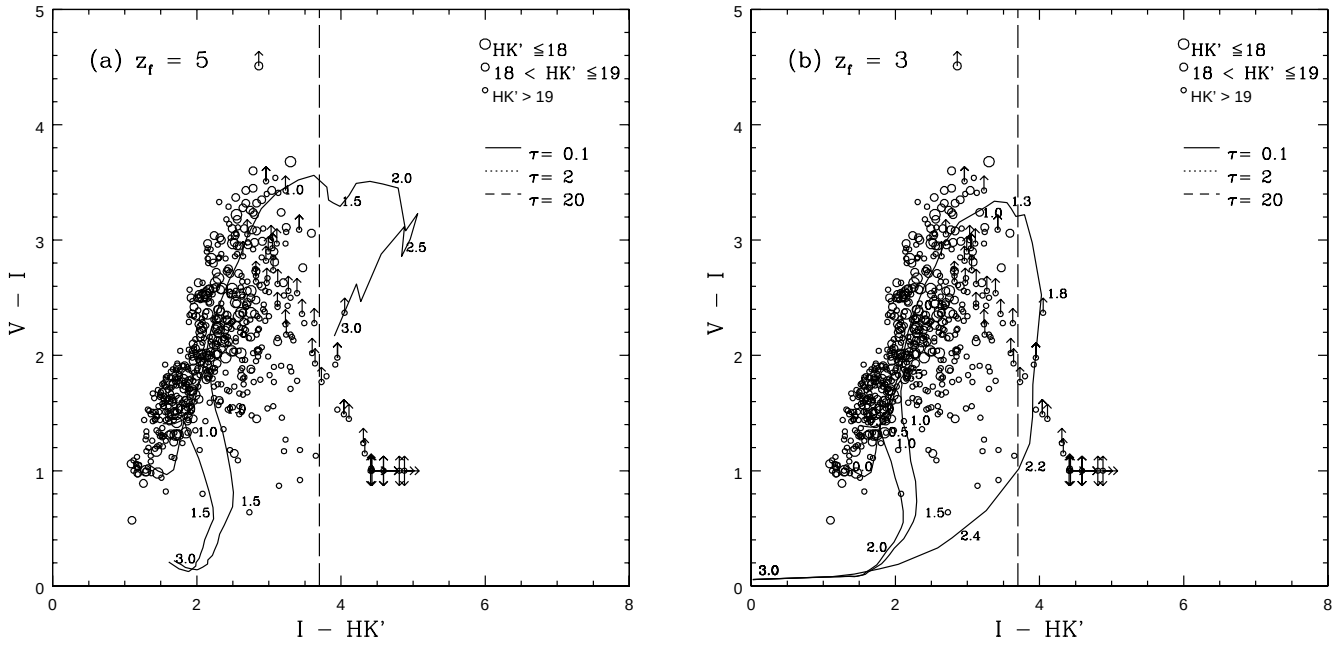

FIG. 4.—$V-I$ vs. $I-HK'$ color-color diagrams for the wide-field $HK' \leq 20.4$ sample (stars have been removed). The BC96 passively evolving model tracks folded with the appropriate V, I, and HK' filters are illustrated from $0 < z < 3$, assuming an epoch of galaxy formation of (*a*) $z_f = 5$ and (*b*) $z_f = 3$. The model tracks have been labeled with a few representative redshifts at which the various colors would be observed. The vertical dashed lines in the figures illustrate the ultrared dividing line, $I-HK' > 3.7$.

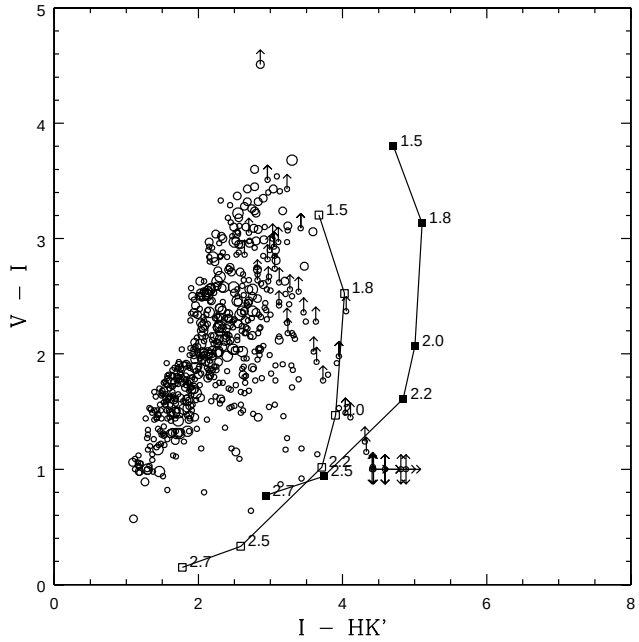

FIG. 5.—The effects of reddening on the $\tau = 0.1$ passive evolution model of BC96 in the $V-I$ vs. $I-HK'$ plane for $z_f = 3$ using the Calzetti (1997) dust attenuation law and a color excess of $E(B-V) = 0.3$. Solid squares represent the reddened SED colors and open squares the intrinsic SED colors. The symbols are labeled with the redshifts of the galaxies that have those colors. The data are from the wide-field sample.

model will approximate an elliptical galaxy SED after about 2 Gyr; if a galaxy formed at $z_f = 3$ in our cosmology, it would not look like an elliptical galaxy until a redshift of $z \sim 1.3$. It is evident from Figure 5 that the reddened elliptical model with $z_f = 3$ could adequately explain the population of galaxies at $I-HK' > 3.7$. Thus, the ultrared population could be a population of dust-enshrouded elliptical galaxies at $z \sim 2$ in the process of formation.

4. CONSTRAINTS ON HIGH-REDSHIFT FIELD ELLIPTICAL GALAXIES

Kauffmann (1996) showed that for a standard cold dark matter (CDM) model with density parameter $\Omega = 1$ and normalization parameter $\sigma_8 = 0.7$ ($b \equiv 1/\sigma_8$), the global number density of bright elliptical galaxies at $z = 1$ is smaller by a factor of 2–3 than that at $z = 0$. Later Kauffmann, Charlot, & White (1996) applied the Schmidt $V/V_{\max}$ test to the color-selected $0.1 < z < 1$ early-type galaxy population in the Canada-France Redshift Survey and found that the observational data were *also* inconsistent with the standard model of passive evolution. The density evolution observed was so strong that it implied that at $z = 1$ only a third of the bright early-type galaxies were already assembled and had the colors of old, passively evolving systems. These authors hence inferred that an increasing fraction of the early-type galaxy population drops out of the sample with increasing redshift, either because they are no longer single units or because star formation has altered their colors. Lilly et al. (1995) had analyzed the same data set previously, however, and had come to the conclusion that there had been no significant evolution.

As discussed in the introduction, an alternative approach is to place an upper limit on the number density of high-redshift evolved elliptical galaxies using very deep imaging at optical and near-infrared wavelengths. The present very large area survey allows us to place limits on the population of $z > 1$ galaxies having ultrared optical–near-IR colors. In order to compare our results with previous K-band surveys, we convert our HK' magnitudes to equivalent K-band magnitudes calculated from the calibration equation $K = HK' - 0.30$ determined in § 2.1. The reddest color convincingly detected in our wide-field sample is $I-K = 4.7 \pm 0.3$. This is comparable to the reddest color reported in the $K \leq 20$ sample of Cowie et al. (1994), $I-K = 5.1 \pm 0.4$. Within the 61.8 arcmin^2 wide-field area we have surveyed ($K \leq 20.1$), we detect only 16 galaxies with galaxy colors $I-K > 4$. In the 7.8 arcmin^2 area of our deep HDF survey ($K \leq 21.2$), we detect four galaxies with colors $I-K > 4$; there are, however, an additional five galaxies with only 2 σ limits on their I magnitudes that could move into the ultrared region. In Table 1, we compare the fraction of objects (12 out of 290) with $I-K > 4$ in the inclusive magnitude range $K = 19$–20 in our wide-field sample and the fraction of objects (four to nine out of 81) with $I-K > 4$ in the inclusive magnitude range $K = 20$–21 in our deep sample with the results of Cowie et al. (1994). Because of improved photometric errors and our much larger area coverage, our wide-field determination of the fraction of ultrared galaxies in the range $K = 19$–20 is expected to be more reliable than that obtained from smaller fields by Cowie et al. (1994). Our improved I-band data may also be responsible for the fact that we find a smaller fraction of ultrared objects in our small field $K = 20$–21 sample than Cowie et al., although this discrepancy could also be a galaxy clustering effect.

We can use our data to place a limit on the number of present-day elliptical galaxies that could have formed in an early burst at high redshift. To do this we need to calculate the space density of ultrared galaxies in our wide-field sample and compare it with the space density of local elliptical galaxies to the same magnitude limit. We assume the ultrared galaxies in our wide-field survey are distributed within the redshift range $1.3 < z < 2.2$, corresponding to a late formation $z_f = 3$ (Fig. 4*b*), in order to estimate the volume for our assumed cosmology ($q_0 = 0.5$ with $H_0 = 50$ km s^{-1} Mpc^{-1}). A higher z_f would give a larger volume and hence a tighter constraint. We find the space density, $n_{\rm ultrared} = N_{\rm obs}/V$, of the ultrared population to be $n_{\rm ultrared} \simeq 1 \times 10^{-4}\, h_{50}^3$ Mpc^{-3} (where h_{50} is a dimensionless quantity: $h_{50} = H_0/50$). This value is to be compared with the local number density, given by the relation

$$n = \phi^*_{50}\, h_{50}^3\, \Gamma(1 + \alpha, \beta)\,, \tag{4}$$

where $\Gamma(1 + \alpha, \beta)$ is the incomplete gamma function with

$$\beta = 10^{-0.4(M_{\rm min} - M^*)} \tag{5}$$

(Yoshii & Takahara 1988) and α is the faint-end slope parameter of the Schechter luminosity function (Schechter 1976). At the limit of our wide-field sample, $K = 20.1$, a galaxy at a mean redshift of $\bar{z} = 1.75$ would have an absolute magnitude $M_{\rm min} = M_K = -23.4 + 5 \log h_{50}$, after including passive evolution and K-corrections derived from a BC96 $\tau = 0.1$ model ($z_f = 3$, $q_0 = 0.5$). At present no local K-band luminosity functions by morphological type have been determined for the field. Therefore, we convert the

TABLE 1

FRACTION OF $I-K>4$ GALAXIES

K (mag)	CURRENT PAPER		COWIE ET AL. 1994	
	Fraction	$\pm 1\ \sigma$ Range	Fraction	$\pm 1\ \sigma$ Range
19–20.....	0.041	0.030–0.057	0.07	0.025–0.14
20–21.....	0.049–0.11	0.026–0.16	0.20	0.15–0.27

B-band pure-elliptical luminosity function parameterization of Marzke et al. (1994) [$M_B^* = -19.23 + 5 \log h_{100}$, $\alpha = -0.85$, and $\phi_{100}^* = (1.5 \pm 0.4) \times 10^{-3}$ Mpc^{-3}] into a K-band elliptical luminosity function using the $B-K$ color of an elliptical galaxy at $z = 0$ ($B-K = 4.43$; Huang, Cowie, & Luppino 1998). This gives $M_K^* = -25.16 + 5 \log h_{50}$ and $\phi_{50}^* = 1.9 \times 10^{-4}$ Mpc^{-3}. Using equations (4) and (5), we estimate the local elliptical galaxy space density to be $n_{\rm local} \simeq 2 \times 10^{-4} h_{50}^3$ Mpc^{-3}. These results indicate that the space density of the ultrared population is $\sim 50\%$ of the space density of the local field elliptical population with $M_K < -23.4$.

It is important to be aware of possible sources of systematic errors in this calculation. First, the comoving volume needed for the ultrared number density calculation depends on the model estimates of the redshift range over which $I-K>4$; the volume would be larger and $n_{\rm ultrared}$ correspondingly smaller for $z_f > 3$. Second, the normalization of the density of the present-day luminosity function is not fully settled, with other surveys giving values that differ from the one we have used by $\pm 25\%$ (see, e.g., the discussion in Huang et al. 1998). Third, a comparison with a local K-band pure-elliptical luminosity function would be preferable to the above conversion of a B-band pure-elliptical luminosity function; such a luminosity function should soon be available (J.-S. Huang 1998, private communication). Fourth, the fraction of ultrared objects is mildly dependent on cosmology; the above calculation, when repeated for a $q_0 = 0.15$ cosmology with $H_0 = 65$ km s^{-1} Mpc^{-1}, gives about a 10% lower ratio of $n_{\rm ultrared}/n_{\rm local}$, so our $q_0 = 0.5$ calculation is conservative in this regard. Fifth, the possibility of reddening in the high-redshift sample should also be considered. If we assume that the possible reddening discussed in § 3 applies to the entire ultrared population but not to the local population, then we find that the ratio increases by about 15%. Finally, although our results are from a large area survey, they are still based on a single field. This introduces a statistical uncertainty associated with field-to-field variations, particularly in a population as small as the ultrared population. Results of other upcoming deep K-band surveys (e.g., papers in preparation by McCracken et al., Eisenhardt et al., and Barger et al.) will be useful in examining this issue.

5. SUMMARY

We have presented wide-field V, I, and HK' images of the Hubble Deep Field and flanking fields, as well as a deeper HK' image of the Hubble Deep Field. Most of the objects in our sample fall within the expected regions of the $V-I$ versus $I-HK'$ color-color plane for blue galaxies at a range of redshifts or red elliptical galaxies at $z < 1$. Significantly, no galaxies are found to follow the track of a pure K-correction elliptical at $z > 1$ in either of our two samples. The track of a passive evolution model with a redshift of formation $z_f = 3$ roughly describes the envelope of the galaxy population in the $V-I$ versus $I-HK'$ plane, except for a very small population of red outliers that could be dusty elliptical galaxies in the process of formation. To an equivalent $K = 20.1$ limit over a large 61.8 arcmin^2 area, we find a surface density for $I-K>4$ objects of 900^{1200}_{700} deg^{-2}, which indicates that this type of object is even more rare than previous small area surveys have suggested. Since an $I-K>4$ color could be mimicked by a highly reddened low-redshift galaxy, this is effectively an upper limit on the population of $z > 1$ ultrared galaxies, provided that there is not a population of completely dust-obscured high-redshift galaxies. We find that the space density of the ultrared galaxies is only a fraction of the estimated space density of present-day field elliptical galaxies with $M_K < -23.4$, and hence we infer that not all local field elliptical galaxies could have formed in single bursts at high redshift.

We thank William Vacca for helpful interactions during the course of this work and Richard Ellis, Roberto Abraham, and Felipe Menanteau for discussions on related research. We thank the anonymous referee for helpful comments. This work was supported by grant AR06377.06-94A from Space Telescope Science Institute, which is operated by AURA, Inc., under NASA contract NAS5-26555. A. J. B. also acknowledges support from NASA through contract P423274 from the University of Arizona, under NASA grant NAG5-3042.

REFERENCES

Aragón-Salamanca, A., Ellis, R. S., Couch, W. J., & Carter, D. 1993, MNRAS, 262, 764
Baugh, C. M., Cole, S., & Frenk, C. S. 1996, MNRAS, 283, 1361
Bertin, E., & Arnouts, S. 1996, A&AS, 117, 393
Calzetti, D. 1997, in AIP Conf. Proc. 408, The Ultraviolet Universe at Low and High Redshift, ed. H. Waller, M. N. Fanelli, J. E. Hollis, & A. C. Danks (New York: AIP), 403
Cimatti, A., Andreani, P., Röttgering, H., & Tilanus, R. 1998, Nature, 392, 895
Cohen, J. G., Blandford, R., Hogg, D. W., Pahre, M. A., & Shopbell, P. L. 1999, ApJ, in press
Cohen, J. G., Cowie, L. L., Hogg, D. W., Songaila, A., Blandford, R., Hu, E. M., & Shopbell, P. 1996, ApJ, 471, L5
Cowie, L. L., Gardner, J. P., Hu, E. M., Songaila, A., Hodapp, K.-W., & Wainscoat, R. J. 1994, ApJ, 434, 114
Eggen, O. J., Lynden-Bell, D., & Sandage, A. R. 1962, ApJ, 136, 748
Ellis, R. S., Smail, I., Dressler, A., Couch, W. J., Oemler, A., Jr., Butcher, H., & Sharples, R. M. 1997, ApJ, 483, 582
Fomalont, E. B., Kellermann, K. I., Richards, E. A., Windhorst, R. A., & Partridge, R. B. 1997, ApJ, 475, 5
Franceschini, A., Silva, L., Fasano, G., Granato, G. L., Bressan, A., Arnouts, S., & Danese, L. 1998, ApJ, 506, 600
Gardner, J. P. 1992, Ph.D. thesis, Univ. Hawaii
Hodapp, K.-W., et al. 1996, NewA, 1, 177
Hogg, D. W., Neugebauer, G., Armus, L., Matthews, K., & Pahre, M. A. 1997, AJ, 113, 2338
Hu, E. M., & Ridgway, S. E. 1994, AJ, 107, 1303
Huang, J.-S., Cowie, L. L., Gardner, J. P., Hu, E. M., Songaila, A., & Wainscoat, R. J. 1997, ApJ, 476, 12
Huang, J.-S., Cowie, L. L., & Luppino, G. A. 1998, ApJ, 496, 31
Kauffmann, G. 1996, MNRAS, 281, 487
Kauffmann, G., & Charlot, S. 1998, MNRAS, 294, 705
Kauffmann, G., Charlot, S., & White, S. D. M. 1996, MNRAS, 283, 117
Kauffmann, G., White, S. D. M., & Guiderdoni, B. 1993, MNRAS, 264, 201
Kelson, D. D., van Dokkum, P. G., Franx, M., Illingworth, G., & Fabricant, D. 1997, ApJ, 478, L13
Kron, R. G. 1980, ApJS, 43, 305
Lilly, S. J., Tresse, L., Hammer, F., Crampton, D., & Le Fèvre, O. 1995, ApJ, 455, 108
Lowenthal, J., Koo, D. C., Guzmán, R., Gallego, J., Phillips, A. C., Faber, S. M., Vogt, N. P., Illingworth, G. D., & Gronwall, C. 1997, ApJ, 481, 673
Marzke, R. O., Geller, M. J., Huchra, J. P., & Corwin, H. G., Jr. 1994, AJ, 108, 437

Moustakas, L. A., Davis, M., Graham, J. R., Silk, J., Peterson, B. A., & Yoshii, Y. 1997, ApJ, 475, 445
Moustakas, L. A., Davis, M., Zepf, S. E., & Bunker, A. J. 1998, in ASP Conf. Ser. 146, The Young Universe: Galaxy Formation and Evolution at Intermediate and High Redshift, ed. S. D'Odorico, A. Fontana, & E. Giallongo (San Francisco: ASP), 210
Phillips, A. C., Guzmán, R., Gallego, J., Koo, D. C., Lowenthal, J. D., Vogt, N. P., Faber, S. M., & Illingworth, G. D. 1997, ApJ, 489, 543
Schechter, P. L. 1976, ApJ, 203, 297
Songaila, A., Cowie, L. L., Hu, E. M., & Gardner, J. P. 1994, ApJS, 94, 461
Stanford, S. A., Eisenhardt, P. R. M., & Dickinson, M. 1995, ApJ, 450, 512
Stanford, S. A., Eisenhardt, P. R., & Dickinson, M. 1998, ApJ, 492, 461
Steidel, C. C., Giavalisco, M., Dickinson, M., & Adelberger, K. 1996, AJ, 112, 352
Tinsley, B. M., & Gunn, J. E. 1976, ApJ, 203, 52
van Dokkum, P. G., & Franx, M. 1996, MNRAS, 281, 985
Wainscoat, R. J., & Cowie, L. L. 1999, in preparation
White, S. D. M., & Frenk, C. S. 1991, ApJ, 379, 52
Williams, R. E., et al. 1996, AJ, 112, 1335
Yoshii, Y., & Takahara, F. 1988, ApJ, 326, 1
Zepf, S. 1997, Nature, 390, 377
Ziegler, B., & Bender, R. 1997, MNRAS, 291, 527